

Binary star influence on post-main-sequence multi-planet stability

Dimitri Veras^{1*}, Nikolaos Georgakarakos², Ian Dobbs-Dixon², Boris T. Gänsicke¹

¹*Department of Physics, University of Warwick, Coventry CV4 7AL, UK*

²*New York University Abu Dhabi, Saadiyat Island, P.O. Box 129188, Abu Dhabi, UAE*

9 March 2021

ABSTRACT

Nearly every star known to host planets will become a white dwarf, and nearly 100 planet-hosts are now known to be accompanied by binary stellar companions. Here, we determine how a binary companion triggers instability in otherwise unconditionally stable single-star two-planet systems during the giant branch and white dwarf phases of the planet host. We perform about 700 full-lifetime (14 Gyr) simulations with A0 and F0 primary stars and secondary K2 companions, and identify the critical binary distance within which instability is triggered at any point during stellar evolution. We estimate this distance to be about seven times the outer planet separation, for circular binaries. Our results help characterize the fates of planetary systems, and in particular which ones might yield architectures that are conducive to generating observable metal pollution in white dwarf atmospheres.

Key words: minor planets, asteroids: general – stars: white dwarfs – methods: numerical – celestial mechanics – planet and satellites: dynamical evolution and stability

1 INTRODUCTION

Single white dwarf planetary systems provide unparalleled insights into planet formation and long-term dynamics. Rocky debris is found in the atmospheres of between one-quarter and one-half of all known single Milky Way white dwarfs (Zuckerman et al. 2003, 2010; Koester et al. 2014). The chemical composition of this debris can be compared directly to solar system asteroid families, and primarily reflect the inner solar system (Gänsicke et al. 2012; Jura & Young 2014; Xu et al. 2014; Wilson et al. 2016). Detected around a few per cent of these “polluted” white dwarfs are dusty circumstellar discs (Farihi et al. 2009; Bergfors et al. 2014; Barber et al. 2016; Farihi 2016) – some of which contain gaseous components (Gänsicke et al. 2006, 2008; Melis et al. 2012; Wilson et al. 2014; Manser et al. 2016) – and one white dwarf (WD 1145+017) features at least one actively disintegrating minor planet (Vanderburg et al. 2015; Alonso et al. 2016; Gänsicke et al. 2016; Gary et al. 2016; Gurri et al. 2016; Rappaport et al. 2016; Redfield et al. 2016; Xu et al. 2016; Veras et al. 2016b; Zhou et al. 2016).

In a system-wide case of pinball (Bonsor & Wyatt 2012), planets are thought to represent a necessary perturbing presence for asteroids, moons or rocky debris to be thrust towards the white dwarf (Bonsor et al. 2011; Debes et al.

2012; Frewen & Hansen 2014; Antoniadou & Veras 2016; Payne et al. 2016a,b; Veras et al. 2016a). As objects encounter the white dwarf Roche, or disruption radius, they break up and form a disc (Graham et al. 1990; Jura 2003; Debes et al. 2012; Bear & Soker 2013; Veras et al. 2014a, 2015a, 2016b) and eventually accrete onto the white dwarf (Bochkarev & Rafikov 2011; Rafikov 2011a,b; Metzger et al. 2012; Rafikov & Garmilla 2012). Although the planets themselves rarely collide with the white dwarf (Veras et al. 2013a; Mustill et al. 2014; Veras & Gänsicke 2015; Veras et al. 2016a; Veras 2016b), they are necessary agents to transport smaller debris towards the star.

The above behaviour need not be restricted to single stars. Circumstellar metal pollution, debris discs and disintegrating asteroids should all occur in some fraction of binary star planetary systems as well (Zuckerman 2014). Planets themselves may be common in binary star systems. Above 140 exoplanets are known to reside in these systems, and about four-fifths of those feature a single planet-host star¹. Although a significant body of work has attempted to understand the formation and evolution of these exoplanets, little attention has been given to their fates (Kratter & Perets 2012; Bonsor & Veras 2015; Hamers & Portegies Zwart 2016; Petrovich & Muñoz 2016). Further, despite the more

* E-mail: d.veras@warwick.ac.uk

¹ <http://exoplanets.org>

common case of exoplanets in “circumstellar” configurations (orbiting one star), the rarer “circumbinary” case (e.g. Doyle et al. 2011; Armstrong et al. 2014; Marsh et al. 2014; Georgakarakos & Eggl 2015) has received the lion’s share of investigations assessing post-main-sequence fate (Sigurdsson 1993; Veras & Tout 2012; Mustill et al. 2013; Portegies Zwart 2013; Schleicher & Dreizler 2014; Völschow et al. 2014; Kostov et al. 2016).

The circumstellar case, in addition to being more common than the circumbinary case, can yield more insights. If binary stars are separated by more than a few tens of au, then they evolve effectively independently of each other. After one of these stars has become a white dwarf, this separation is large enough to ensure that the companion’s wind provides a negligible chemical change to the white dwarf’s atmosphere (Veras, Xu & Rebassa-Mansergas 2016). Consequently, one can link this white dwarf with the characteristics of a single white dwarf planetary system.

Here, we address the dearth of work investigating circumstellar planetary systems within evolved binaries by estimating a stability limit for a relatively simple but important base case. We consider two nearly coplanar planets in each system, as opposed to the single planet cases from Kratter & Perets (2012), Bonsor & Veras (2015) and Hamers & Portegies Zwart (2016), and the high mutual inclinations between the binary star and planetary system in Petrovich & Muñoz (2016). Our focus is also entirely different. Kratter & Perets (2012) detailed how a planet may “hop” from one star to the other during post-main-sequence mass loss, and Bonsor & Veras (2015) illustrated how the combination of Galactic tides and post-main-sequence mass loss conspire to stretch the orbits of stellar binaries such that a previously quiescent planet becomes suddenly dynamically active. Our two planets orbit the same star at distances commensurate with those of solar system giant planets, which precludes star hopping. Our initial binary separation is no greater than 500 au, rendering Galactic tides ineffective.

Consequently, our focus is on the stellar phase-dependent stability of the resulting four-body system. We determine simply the binary separation within which the two-planet system becomes unstable during their host star’s main sequence, giant branch and white dwarf phases, rather than introducing more complex considerations such as Lidov-Kozai oscillations or accretion rate estimations (Hamers & Portegies Zwart 2016; Petrovich & Muñoz 2016). In Section 2 we briefly recapitulate some relevant stability results, before in Section 3 detailing the initial conditions for our simulations. We present our results in Section 4 and conclude in Section 5.

2 STABILITY LIMITS

Unlike the three-body problem, for which many analytic formulations of stability exist (e.g. Georgakarakos 2008), similar concise expressions for four-body problems are rarer (e.g. Loks & Sergysels 1985; Sergysels & Loks 1987), even despite major recent progress with central configuration theory (Érdi & Czirják 2016; Hamilton 2016; Veras 2016c). Further, when one of the bodies loses mass – as is the case for a main-sequence star which becomes a white dwarf – then

not even the two-body problem is solvable (see Chapter 4 of Veras 2016a).

These restrictions persuade us to construct binary systems based on our knowledge of the three-body problem with mass loss. Two-planet systems where the central star evolves into a white dwarf were the focus of investigations by Debes & Sigurdsson (2002), Veras et al. (2013a) and Voyatzis et al. (2013). A key finding from Debes & Sigurdsson (2002) was that two planets which are Hill stable on the main sequence – meaning that their orbits could never cross – might no longer be Hill stable as the central star loses mass. Veras et al. (2013a) then expanded on that work with a wider exploration of parameter space, and by also considering Lagrange stability, which is the dynamical state of two Hill stable planets that remain bounded and ordered. Voyatzis et al. (2013) explored the evolution of two planets in mean motion resonances, and the “non-adiabatic” orbital variations resulting from violent mass loss.

The adiabaticity of a system is defined here as the extent to which its planets’ orbits change in a predictable manner due to stellar mass loss: when the eccentricity variations are negligible and the semimajor axes values increase in direct proportion to the extent of the mass loss. Adiabaticity is quantified by a formula like that of equation (15) of Veras et al. (2011), which represents a scaled ratio of the orbital period to the mass loss timescale. When this ratio is much less than unity, the system is said to be adiabatic. Veras et al. (2011) showed that any stellar companion within several hundred au will evolve adiabatically. The stability boundary changes found by Debes & Sigurdsson (2002) and Veras et al. (2013a) hence considered only the adiabatic state because that corresponds to the expected fate of the majority of currently-known exoplanetary systems.

The Hill stability limit and probably the Lagrange stability limit are scale-free in the sense that they depend on ratios of orbital elements of the planets rather than the explicit planet-star separations themselves (Gladman 1993; Barnes & Greenberg 2006; Donnison 2006; Barnes & Greenberg 2007; Raymond et al. 2009; Veras & Mustill 2013; Marzari 2014; Petrovich 2015). This property is particularly useful for studies such as this one in order to reduce the number of degrees of freedom of the explored systems and to place the planets well-beyond the tidal reach of the evolving star (Villaver & Livio 2009; Kunitomo et al. 2011; Mustill & Villaver 2012; Adams & Bloch 2013; Nordhaus & Spiegel 2013; Villaver et al. 2014; Staff et al. 2016). However, after instability does occur, the problem no longer remains scale-free (Johansen et al. 2012; Petrovich et al. 2014).

Of particular interest here are two-planet systems which are sufficiently Lagrange stable around a single star to survive Gyrs into the white dwarf phase, but not under the influence of a binary companion. Stellar mass loss will expand the orbits of both planets relative to their initial values more than the orbit of the binary companion (even though all expansions are adiabatic; see equation 3 of Kratter & Perets 2012, equations A22-A23 of Petrovich & Muñoz 2016 and equations 7.6-7.7 of Veras 2016a). Consequently, because angular momentum must be conserved (assuming isotropic mass loss), the post-mass-loss state of the system leaves it

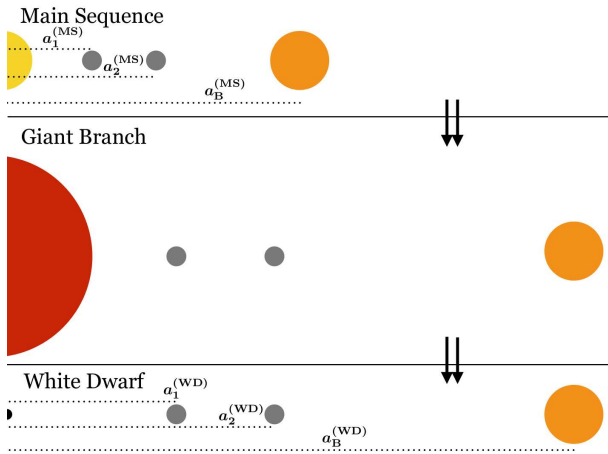


Figure 1. Cartoon (not to scale) of our setup: two planets (small grey circles) orbiting the primary (yellow, red then black star at left), plus a secondary (orange star at right). As the primary evolves from the main sequence (top region) to the giant branch phase (middle region) to the white dwarf phase (bottom region), the star expands and then contracts. Concurrently, the planets and secondary all expand their orbits. This paper explores what binary separations would create instability, and during what phases.

more fragile and susceptible to instability than on the main sequence.

3 INITIAL CONDITIONS

The above considerations motivate our initial conditions, which are measured in Jacobi coordinates. Assume that the primary star is the planet-hosting star and evolves from a main sequence star to a white dwarf. Denote its mass as $M_*(t)$. The two planets it hosts have masses M_1 and M_2 and semimajor axes $a_1(t)$ and $a_2(t)$ such that $a_1(0) < a_2(0)$. The binary stellar companion, which will be denoted as the “secondary”, has mass M_B and a semimajor axis of $a_B(t)$. The secondary’s mass is time-independent because it is assumed (i) to be low enough such that it remains on the main sequence for the duration of our simulations, and (ii) mass loss from main sequence winds is negligible. In Fig. 1, we show a cartoon of the bodies in our simulations and how they would evolve in time in a stable manner.

The large phase space of the four-body problem, combined with the time-consuming nature of the simulations that extend beyond the main sequence, demanded that we carefully chose what parameters to explore. We focused on $a_B(t)$ and minimally sampled variations of other parameters.

3.1 Masses

We fixed $M_1 = M_2 = M_{\text{Jupiter}}$ and $M_B = 0.81M_\odot$, which corresponds to a K2 star by Appendix B of Gray (2008). Using that same table we sampled both A0 stars ($M_* = 2.34M_\odot$) and F0 stars ($M_* = 1.66M_\odot$) for our primary. These choices allowed us to evolve the primary star through all phases of stellar evolution while the secondary remained on the main sequence. The main sequence lifetimes of A0, F0 and K2 stars are respectively, roughly 0.75,

2 and > 20 Gyr; the A0 and F0 stars turn into white dwarfs with masses of about $0.65M_\odot$ and $0.60M_\odot$ (Hurley et al. 2000). Both A0 and F0 stars represent common progenitors of the present-day population of white dwarfs in the Milky Way (e.g. Tremblay et al. 2016).

3.2 Orbits

We set $a_1(0) = 5$ au and sampled three values of $a_2(0)$ corresponding to 8, 10 and 20 times the mutual Hill radius (β), as defined by Smith & Lissauer (2009). For A0 stars, these values correspond to $a_2(0) = 8.50, 9.79, 23.4$ au, whereas for F0 stars, they correspond to $a_2(0) = 9.10, 10.7, 31.5$ au. The resulting semimajor axis ratios are far from any strong orbital period commensurability, and large enough to ensure Hill stability (e.g. Donnison 2006) and probably Lagrange stability (Petrovich 2015), both along the main sequence and white dwarf phases (Veras et al. 2013a). Further, because $M_1/M_*, M_2/M_* \ll 1$ during all phases, the breakdown of these limits for sufficiently high planet masses (Morrison & Kratter 2016) is not consequential here. We then set the planetary initial orbital eccentricities to zero. These choices help us focus on determining the global stability boundary as a function of a_B and not deplete resources by modelling already-unstable two-planet, one-star systems.

We sampled up to eleven different values of a_B for a given set of mass and planetary separations, and adopted the range $50 \text{ au} \leq a_B(0) \leq 500 \text{ au}$. For stability considerations, the absolute value of $a_B(0)$ is not as important as the ratio $a_B(0)/a_2(0)$, through which we report our results. However, the upper bound of $a_B(0)$ is important because it is low enough that we can justify ignoring the effect of Galactic tides and stellar flybys (Veras et al. 2014b). Although our focus was on circular binary orbits, we also performed simulations with nonzero binary eccentricities (e_B) of 0.2, 0.4 and 0.8.

Due to the chaotic nature of long-term evolution simulations of planetary systems, we did not wish to perform just one simulation for each set of masses, semimajor axes and eccentricities sampled. Instead we performed four per set. Within each of the four simulations, for the two planets and the binary companion, we randomly selected, from a uniform distribution, mean anomalies, arguments of pericentre and longitudes of ascending node across their entire ranges, and inclinations between -1° and 1° .² Effectively, both stars and both planets are all nearly coplanar.

3.3 Integrator

In order to simulate system evolution across all stellar phases, we needed to concurrently propagate the orbital evolution of the planets and binary star with the physical evolution of the primary. A currently available tool which is well-suited for this purpose is the modified version of the Bulirsch-Stoer integrator from the `Mercury` integration package (Chambers 1999). The modifications were detailed in Veras et al. (2013a) and involve splicing the mass and radius output from the `SSE` stellar evolution code (Hurley et al.

² This choice helps prevent an artificially high rate of planet-planet collisions; see Mustill et al. (2014).

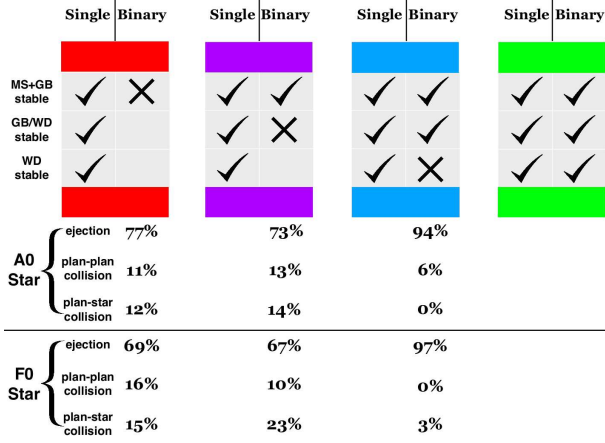


Figure 2. Classification of our results. The designations MS, GB and WD refer to main sequence, giant branch and white dwarf, and “GB/WD stable” refers to the timespan of 10 Myr which bisects the transition point between the two phases. The colours refer to particular configurations which feature instability: *red* for binary system instability on the main sequence or giant branch phase, *purple* for binary system instability during the GB/WD transition, and *blue* for binary system instability during the white dwarf phase. *Green* refers to binary systems which remained stable throughout 14 Gyr of evolution. All single-star planetary systems remained stable over this timespan. The instability statistics below the chart are divided according to whether the primary is an A0 star or F0 star.

2000) within each Burlisch–Stoer substep in order to determine each global timestep.

The consequence is that tens or hundreds of timesteps are needed to resolve a single orbit of the inner planet. Long-term integrations are hence time-consuming. We integrated our simulations for 14 Gyr, which is the current age of the Universe (also known as a Hubble time), and were able to perform a total of about 700 simulations with two stars and two planets. We then repeated all simulations but with the binary star removed. Doing so provided a necessary contrast in order to isolate the binary influence.

Because the primary was treated as a point particle with a variable mass, mass loss is effectively treated as isotropic, a well-used and justified approximation (Veras et al. 2013b). The ejection distance is computed using the Galactic tidal model from Veras & Evans (2013) and assuming that the stars reside at a distance of 8 kpc from the Galactic centre. This ejection boundary takes the form of an ellipsoid, and an ejection was deemed to occur when the code detected that a planet resided outside of this ellipsoid. The ellipsoid itself changes shape as the primary loses mass; this change was tracked by our code. The primary was evolved assuming Solar metallicity, a Reimers mass loss numerical coefficient of $2 \times 10^{-13} M_{\odot} \text{ yr}^{-1}$ for the classic prescription Kudritzki & Reimers (1978), and, along the asymptotic giant branch, the superwind prescription of Vassiliadis & Wood (1993).

4 RESULTS

Our goal is to link binary separation with stability. We define an unstable system as one which has experienced an

ejection or collision. In our simulations, the collisions occurred either between two planets or between a planet and the primary (the planetary radius was equivalent to that of Jupiter and the stellar radii were given by *SSE*). Only planets were ever ejected: all secondaries remained bound to the primary. Every one of our set of simulations with no secondary remained stable for 14 Gyr, providing a useful point of comparison and confirming that our choices of $a_1(0)$ and $a_2(0)$ were Lagrange-stable in the single-star case.

4.1 Instability classification

We classified simulation outcomes according to four types, which are displayed in Fig. 2. Each type is colour-coded for easy linkage to our main result, which is presented in Fig. 3. The types are: (green) stable throughout the simulation; (blue) stable until some point along the white dwarf stage; (purple) stable until the transition period between the end of the giant branch and start of the white dwarf phase; (red) unstable during the main sequence or giant branch phases. We define the transition period as the 10 Myr span which is bisected by the exact time when the star becomes a white dwarf (964 Myr for A0 stars and 2270 Myr for F0 stars, according to Hurley et al. 2000). This transition period includes the tip of the asymptotic giant branch, where the “superwind” (Lagadec & Zijlstra 2008) is strongest. Consequently, instability is common during this time (e.g. see Appendix A of Veras et al. 2016a). In contrast, the transition between the main sequence and giant branch phases is gradual and not dynamically noteworthy.

The instability fractions given in Fig. 2 indicate that the majority of instability in all cases occurs in the form of ejections. This fraction is above 90 per cent for systems which become unstable during the white dwarf phase. Just a few per cent of white dwarf unstable systems feature planet-primary collisions, although this value might be an underestimate because no tidal effects were included in the simulations, and because collisions were determined according to the actual white dwarf radius as opposed to its Roche, or disruption, radius. Those fractions are further slightly blighted by small number statistics (90 total blue instabilities, as opposed to 148 red and 217 purple ones).

4.2 Main result

Our main result, in Fig. 3, illustrates when instability occurs in binary separation space. Each square represents the mean outcome of four sets of simulations run with different mean anomalies, longitudes of pericentre and arguments of ascending node. The mean is computed by a colour-blend of the four outcomes, where the colours associated with each outcome are illustrated in Fig. 2. The bubble in the upper-left corner of each plot indicates the primary stellar type, and the initial separation of planets in mutual Hill radii (β).

Overall, the figure illustrates a trend from red (main sequence instability) to green (stability) as the binary separation increases, an expected result. Because the colour trend is not strictly monotonic (e.g. left side of the upper-rightmost plot) and computational limitations prevent us from covering the entire phase space, we cannot identify specific values of $a_B(0)/a_2(0)$ for which transitions in behaviour

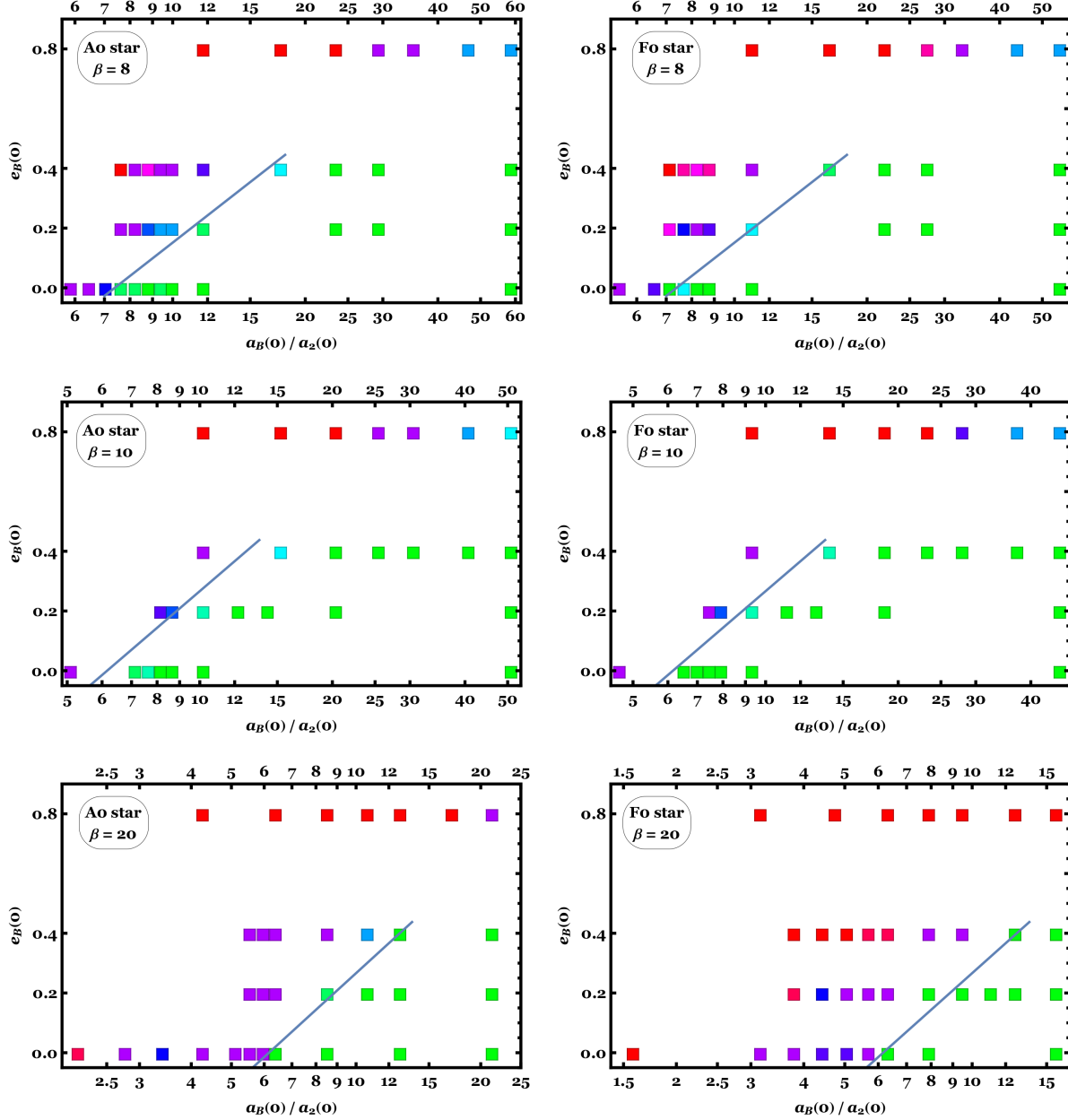


Figure 3. Stability limits (*red*: unstable on main sequence or giant branch phases; *purple*: unstable during the giant branch / white dwarf transition; *blue*: unstable on white dwarf phase; *green*: stable throughout). The squares represent colour-blended outcomes (see Fig. 2) of sets of four simulations run with different initial orbital angles and small inclinations. The diagonal lines correspond to rough empirical estimates (equation 1) for the transition between green squares and the other squares. The left and right panels, which are consistent with one another, respectively contain A0 and F0 primary stars. In all panels, $a_1(0) = 5$ au; the top, middle and bottom panels have, for A0 primary stars, $a_2(0) = 8.50, 9.79, 23.4$ au, and for F0 primary stars, $a_2(0) = 9.10, 10.7, 31.5$ au. These values correspond to mutual Hill radii separations of $\beta = 8, 10$ and 20 . The plots suggest that (i) for circular binaries, $a_B(0)/a_2(0) > 7$ nearly ensures stability, and (ii) for highly eccentric binaries, the good colour resolution over a wide range of $a_B(0)/a_2(0)$ allows one to more easily generate instability at a desired phase for a given set of initial conditions.

occur. Nevertheless, we can still establish some fairly robust estimates.

Consider first the case for circular binaries. In all cases the systems are stable for $a_B(0)/a_2(0) \gtrsim 10$, and probably $a_B(0)/a_2(0) \gtrsim 7$ given the bounding $\beta = 8$ and $\beta = 20$ cases. If not stable, then the system is likely to survive over the entire main sequence and giant branch phases, but is

unlikely to survive intact well into the white dwarf phase: the transition from giant branch star into a white dwarf triggers instability unless $a_B(0)/a_2(0) > 3$.

The same relations cannot be used for more eccentric binary cases. The critical separation for stability across all phases increases with increasing $e_B(0)$. For moderate eccentricity cases ($e_B(0) = 0.2, 0.4$) and $\beta \leq 10$, stability is al-

ways achieved for $a_B(0)/a_2(0) \gtrsim 60$. In contrast, for this semimajor axis ratio and $e_B(0) = 0.8$, instability is achieved predominately along the white dwarf phase. Highly eccentric binaries appear to stretch out the instability regimes across a wider swath of $a_B(0)/a_2(0)$ space, which fortuitously allows one to more easily select initial conditions with predictable outcomes.

In order to aid estimation of the phase space region where the transition from stable (green) to unstable (all other colours) occurs for non-zero binary eccentricity, we provide rough empirical estimates in equation form. We find that stability is achieved if the following is satisfied:

$$e_B(0) < \begin{cases} 0.50 \ln \left[\frac{a_B(0)}{a_2(0)} \right] - 1 & \text{if } \beta = 8, \\ 0.55 \ln \left[\frac{a_B(0)}{a_2(0)} \right] - 1 & \text{if } \beta = 10, 20 \end{cases} \quad (1)$$

for $0.0 < e_B(0) \leq 0.4$. We have drawn these curves on all of the plots in Fig. 3.

We can also compare results for both types of primary star studied (left and right panels). The agreement is good enough in nearly all cases (but not necessarily the $\beta = 20$, $e_B(0) = 0.4$ case) to conclude that the stability limits change little depending on which type of star in the A-F spectral type range which is used. This robustness provides evidence that adopting a single primary mass may be sufficient for future investigations.

4.3 Eccentricity evolution

Instability in multi-planet systems, partly through eccentricity generation, may easily yield configurations which can lead to white dwarf pollution, as detailed by Veras et al. (2013a), Mustill et al. (2014), Veras & Gänsicke (2015), Payne et al. (2016a), Payne et al. (2016b), Veras (2016b), and Veras et al. (2016a). However, what about simulations which remain stable throughout all stellar phases but are still perturbed due to the presence of a secondary? In the single-star case, Figure 8 of Mustill et al. (2014) illustrates that for their stable simulations, mutual interactions of three planets during mass loss can raise eccentricities up to 0.2. Voyatzis et al. (2013) used a different integrator and found that eccentricity variations can easily reach several tenths (see, in particular, their figs. 16-17).

Here, our green-coloured simulations allow us to evaluate how high the planetary eccentricities become on the white dwarf phase for stable simulations. We find that in extreme cases, planet eccentricities can reach values of about 0.1 from main sequence maximum values of 0.01. Our more muted excitation probably arises from the fact that we have adopted much less massive stars than Voyatzis et al. (2013) and Mustill et al. (2014), who partly used particularly violent and rare $8M_\odot$ (B2) primary stars. Further, if our secondary was too far away to ever trigger instability, then its effect on the planetary eccentricity was not great enough to raise it to 0.1. Analytical explanations for three-body (and four-body) dynamics during stellar mass loss is sorely in

need of future exploration, and appears to not represent a simple extension of two-body dynamics.³

Whatever eccentricity excitation occurs during mass loss, after the star has become a white dwarf, then the system again becomes a fixed-mass system for which other theories may be applicable. One option is Laplace-Lagrange secular theory (Chapter 7 of Murray & Dermott 1999), which is sufficient for a first evaluation of the dynamics of a system. However, this theory is of low order in the masses, eccentricities and semimajor axis ratio a_1/a_2 . Hence, it may give reasonable results for problems in our Solar System but typically not in exoplanetary systems (where eccentricities may be high and semimajor axis ratios small) or for planets in stellar binaries. In that latter case, there are several studies that perform expansions to second order in the masses and develop solutions for higher values in the eccentricities and in the semimajor axis ratio (e.g. Georgakarakos 2002, 2003; Libert & Henrard 2005; Georgakarakos 2006; Libert & Henrard 2006; Veras & Armitage 2007; Georgakarakos 2009; Giuppone et al. 2011; Libert & Sansottera 2013; Georgakarakos et al. 2016), which can describe the dynamics of the system more accurately. Of course, as the above studies refer to three-body systems, they could only be used if our four-body system could be approximated by a three-body one (as for example where the companion star is sufficiently distant to be considered as having a negligible influence on the orbital evolution of the two planets).

5 CONCLUSION

Motivated by the fact that planetary origins of metal pollution in white dwarf atmospheres are not necessarily limited to single white dwarfs (Zuckerman 2014), we have probed stability limits in evolving circumstellar two-planet systems with non-evolving secondaries. We found that for circular binaries, if the planets are sufficiently far from their parent star to avoid engulfment on the giant branch phase, then $a_B(0)/a_2(0) \gtrsim 7$ ensures stability across all phases of stellar evolution. Instability during the white dwarf phase occurs for an increasing spread of $a_B(0)/a_2(0)$ values as e_B increases. Our results (Fig. 3) (i) provide useful benchmarks from which one could set up simulations that generate instability along particular phases, (ii) display phase space portraits which can be compared to observed systems, and (iii) represent a starting point for explorations of more complex architectures with asteroids, moons, additional planets and/or significantly inclined bodies.

ACKNOWLEDGEMENTS

We thank the referee, Cristobal Petrovich, for his insightful and probing feedback, which has improved the manuscript.

³ Two-body dynamics, from equations 15 and 17 of Veras et al. (2011), indicates that the mass-loss induced eccentricity jump for our simulations would be on the order of just 10^{-4} . In this situation, there are no multi-planet interactions.

DV and BTG have received funding from the European Research Council under the European Union's Seventh Framework Programme (FP/2007-2013)/ERC Grant Agreement n. 320964 (WDTracer). We would like to thank the High Performance Computing Resources team at New York University Abu Dhabi and especially Jorge Naranjo for helping us carry out our simulations.

REFERENCES

- Adams, F. C., & Bloch, A. M. 2013, *ApJL*, 777, L30
- Alonso, R., Rappaport, S., Deeg, H. J., & Palles, E. 2016, *A&A*, 589, L6
- Antoniadou, K. I., & Veras, D. 2016, *MNRAS*, In Press, arXiv:1609.01734
- Armstrong, D. J., Osborn, H. P., Brown, D. J. A., et al. 2014, *MNRAS*, 444, 1873
- Barber, S. D., Belardi, C., Kilic, M., & Gianninas, A. 2016, *MNRAS*, 459, 1415
- Barnes, R., & Greenberg, R. 2006, *ApJL*, 647, L163
- Barnes, R., & Greenberg, R. 2007, *ApJL*, 665, L67
- Bear, E., & Soker, N. 2013, *New Astronomy*, 19, 56
- Bergfors, C., Farihi, J., Dufour, P., & Rocchetto, M. 2014, *MNRAS*, 444, 2147
- Bochkarev, K. V., & Rafikov, R. R. 2011, *ApJ*, 741, 36
- Bonsor, A., Mustill, A. J., & Wyatt, M. C. 2011, *MNRAS*, 414, 930
- Bonsor, A., & Wyatt, M. C. 2012, *MNRAS*, 420, 2990
- Bonsor, A., & Veras, D. 2015, *MNRAS*, 454, 53
- Chambers, J. E. 1999, *MNRAS*, 304, 793
- Debes, J. H., & Sigurdsson, S. 2002, *ApJ*, 572, 556
- Debes, J. H., Walsh, K. J., & Stark, C. 2012, *ApJ*, 747, 148
- Donnison, J. R. 2006, *MNRAS*, 369, 1267
- Doyle, L. R., Carter, J. A., Fabrycky, D. C., et al. 2011, *Science*, 333, 1602
- Érdi, B., & Czirják, Z. 2016, *Celestial Mechanics and Dynamical Astronomy*, 125, 33
- Farihi, J., Jura, M., & Zuckerman, B. 2009, *ApJ*, 694, 805
- Farihi, J. 2016, *New Astronomy Reviews*, 71, 9
- Frewen, S. F. N., & Hansen, B. M. S. 2014, *MNRAS*, 439, 2442
- Gänsicke, B. T., Marsh, T. R., Southworth, J., & Rebassamansergas, A. 2006, *Science*, 314, 1908
- Gänsicke, B. T., Koester, D., Marsh, T. R., Rebassamansergas, A., & Southworth, J. 2008, *MNRAS*, 391, L103
- Gänsicke, B. T., Koester, D., Farihi, J., et al. 2012, *MNRAS*, 424, 333
- Gänsicke, B. T., Aungwerojwit, A., Marsh, T. R., et al. 2016, *ApJL*, 818, L7
- Gary, B. L., Rappaport, S., Kaye, T. G., Alonso, R., & Hamsch, F.-J. 2016, Submitted to *MNRAS*, arXiv:1608.00026
- Georgakarakos, N. 2002, *MNRAS*, 337, 559
- Georgakarakos, N. 2003, *MNRAS*, 345, 340
- Georgakarakos, N. 2006, *MNRAS*, 366, 566
- Georgakarakos, N. 2008, *Celestial Mechanics and Dynamical Astronomy*, 100, 151
- Georgakarakos, N. 2009, *MNRAS*, 392, 1253
- Georgakarakos, N., & Eggl, S. 2015, *ApJ*, 802, 94
- Georgakarakos, N., Dobbs-Dixon, I., & Way, M. J. 2016, *MNRAS*, In Press
- Giuppone, C. A., Leiva, A. M., Correa-Otto, J., & Beaugé, C. 2011, *A&A*, 530, A103
- Gladman, B. 1993, *Icarus*, 106, 247
- Graham, J. R., Matthews, K., Neugebauer, G., & Soifer, B. T. 1990, *ApJ*, 357, 216
- Gray, D. F. 2008, *The Observation and Analysis of Stellar Photospheres*. Cambridge, UK: Cambridge University Press.
- Gurri, P., Veras, D., & Gänsicke, B. T. 2016, *MNRAS*, In Press, arXiv:1609.02563
- Hamers, A. S., & Portegies Zwart, S. F. 2016, *MNRAS*, 462, L84
- Hamilton, D. P. 2016, *Nature*, 533, 187
- Hurley, J. R., Pols, O. R., & Tout, C. A. 2000, *MNRAS*, 315, 543
- Johansen, A., Davies, M. B., Church, R. P., & Holmelin, V. 2012, *ApJ*, 758, 39
- Jura, M. 2003, *ApJL*, 584, L91
- Jura, M., & Young, E. D. 2014, *Annual Review of Earth and Planetary Sciences*, 42, 45
- Koester, D., Gänsicke, B. T., & Farihi, J. 2014, *A&A*, 566, A34
- Kostov, V. B., Moore, K., Tamayo, D., Jayawardhana, R., & Rinehart, S. A. 2016, *ApJ* In Press, arXiv:1610.03436
- Kratter, K. M., & Perets, H. B. 2012, *ApJ*, 753, 91
- Kudritzki, R. P., & Reimers, D. 1978, *A&A*, 70, 227
- Kunitomo, M., Ikoma, M., Sato, B., Katsuta, Y., & Ida, S. 2011, *ApJ*, 737, 66
- Lagadec, E., & Zijlstra, A. A. 2008, *MNRAS*, 390, L59
- Libert, A.-S., & Henrard, J. 2005, *Celestial Mechanics and Dynamical Astronomy*, 93, 187
- Libert, A.-S., & Henrard, J. 2006, *Icarus*, 183, 186
- Libert, A.-S., & Sansottera, M. 2013, *Celestial Mechanics and Dynamical Astronomy*, 117, 149
- Loks, A., & Sergysels, R. 1985, *A&A*, 149, 462
- Manser, C. J., Gänsicke, B. T., Marsh, T. R., et al. 2016, *MNRAS*, 455, 4467
- Marsh, T. R., Parsons, S. G., Bours, M. C. P., et al. 2014, *MNRAS*, 437, 475
- Marzari, F. 2014, *MNRAS*, 442, 1110
- Melis, C., Dufour, P., Farihi, J., et al. 2012, *ApJL*, 751, L4
- Metzger, B. D., Rafikov, R. R., & Bochkarev, K. V. 2012, *MNRAS*, 423, 505
- Morrison, S. J., & Kratter, K. M. 2016, *ApJ*, 823, 118
- Murray, C. D., & Dermott, S. F. 1999, *Solar system dynamics*
- Mustill, A. J., & Villaver, E. 2012, *ApJ*, 761, 121
- Mustill, A. J., Marshall, J. P., Villaver, E., et al. 2013, *MNRAS*, 436, 2515
- Mustill, A. J., Veras, D., & Villaver, E. 2014, *MNRAS*, 437, 1404
- Nordhaus, J., & Spiegel, D. S. 2013, *MNRAS*, 432, 500
- Payne, M. J., Veras, D., Holman, M. J., Gänsicke, B. T. 2016a, *MNRAS*, 457, 217
- Payne, M. J., Veras, D., Gänsicke, B. T., Holman, M. J. 2016b, *MNRAS* In Press, arXiv:1610.01597
- Petrovich, C., Tremaine, S., & Rafikov, R. 2014, *ApJ*, 786, 101
- Petrovich, C. 2015, *ApJ*, 808, 120
- Petrovich, C., & Muñoz, D. J. 2016, Submitted to *AAS*

- Journals, arXiv:1607.04891
- Portegies Zwart, S. 2013, MNRAS, 429, L45
- Rafikov, R. R. 2011a, MNRAS, 416, L55
- Rafikov, R. R. 2011b, ApJL, 732, L3
- Rafikov, R. R., & Garmilla, J. A. 2012, ApJ, 760, 123
- Rappaport, S., Gary, B. L., Kaye, T., et al. 2016, MNRAS, 458, 3904
- Raymond, S. N., Barnes, R., Veras, D., et al. 2009, ApJL, 696, L98
- Redfield, S., Farihi, J., Cauley, P. W., et al. 2016, Submitted to ApJ, arXiv:1608.00549
- Schleicher, D. R. G., & Dreizler, S. 2014, A&A, 563, A61
- Sergysels, R., & Loks, A. 1987, A&A, 182, 163
- Sigurdsson, S. 1993, ApJL, 415, L43
- Smith, A. W., & Lissauer, J. J. 2009, Icarus, 201, 381
- Staff, J. E., De Marco, O., Wood, P., Galaviz, P., & Passy, J.-C. 2016, MNRAS, 458, 832
- Tremblay, P.-E., Cummings, J., Kalirai, J. S., et al. 2016, MNRAS, 461, 2100
- Vanderburg, A., Johnson, J. A., Rappaport, S., et al. 2015, Nature, 526, 546
- Vassiliadis, E., & Wood, P. R. 1993, ApJ, 413, 641
- Veras, D., & Armitage, P. J. 2007, ApJ, 661, 1311
- Veras, D., Wyatt, M. C., Mustill, A. J., Bonsor, A., & Eldridge, J. J. 2011, MNRAS, 417, 2104
- Veras, D., & Tout, C. A. 2012, MNRAS, 422, 1648
- Veras, D., Mustill, A. J., Bonsor, A., & Wyatt, M. C. 2013a, MNRAS, 431, 1686
- Veras, D., Hadjidemetriou, J. D., & Tout, C. A. 2013b, MNRAS, 435, 2416
- Veras, D., & Evans, N. W. 2013, MNRAS, 430, 403
- Veras, D., & Mustill, A. J. 2013, MNRAS, 434, L11
- Veras, D., Leinhardt, Z. M., Bonsor, A., Gänsicke, B. T. 2014a, MNRAS, 445, 2244
- Veras, D., Evans, N. W., Wyatt, M. C., & Tout, C. A. 2014b, MNRAS, 437, 1127
- Veras, D., Gänsicke, B. T. 2015, MNRAS, 447, 1049
- Veras, D., Leinhardt, Z. M., Eggl, S., Gänsicke, B. T. 2015a, MNRAS, 451, 3453
- Veras, D. 2016a, Royal Society Open Science, 3, 150571
- Veras, D. 2016b, MNRAS, 463, 2958
- Veras, D. 2016c, MNRAS, 462, 3368
- Veras, D., Mustill, A. J., Gänsicke, B. T., et al. 2016a, MNRAS, 458, 3942
- Veras, D., Carter, P. J., Leinhardt, Z. M., Gänsicke, B. T., et al. 2016b, Submitted to MNRAS
- Veras, D., Xu, S., Rebassa-Mansergas 2016, In Prep
- Villaver, E., & Livio, M. 2009, ApJL, 705, L81
- Villaver, E., Livio, M., Mustill, A. J., & Siess, L. 2014, ApJ, 794, 3
- Völschow, M., Banerjee, R., & Hessman, F. V. 2014, A&A, 562, A19
- Voyatzis, G., Hadjidemetriou, J. D., Veras, D., & Varvoglis, H. 2013, MNRAS, 430, 3383
- Wilson, D. J., Gänsicke, B. T., Koester, D., et al. 2014, MNRAS, 445, 1878
- Wilson, D. J., Gänsicke, B. T., Farihi, J., & Koester, D. 2016, MNRAS, 459, 3282
- Xu, S., Jura, M., Koester, D., Klein, B., & Zuckerman, B. 2014, ApJ, 783, 79
- Xu, S., Jura, M., Dufour, P., & Zuckerman, B. 2016, ApJL, 816, L22
- Zhou, G., Kedziora-Chudczer, L., Bailey, J., et al. 2016, submitted to MNRAS, arXiv:1604.07405
- Zuckerman, B., Koester, D., Reid, I. N., Hüensch, M. 2003, ApJ, 596, 477
- Zuckerman, B., Melis, C., Klein, B., Koester, D., & Jura, M. 2010, ApJ, 722, 725
- Zuckerman, B. 2014, ApJL, 791, L27